ICAS 2021 SHANGHAI
International Council of the Aeronautical Sciences
32nd Congress of the International Council of the Aeronautical Sciences
September 6-10, 2021
Pudong Shangri-La, Shanghai, China

ADJOINT–BASED STUDY OF THE AERODYNAMIC CENTER SHIFT IN THE TRANSONIC FLOW REGIME

Arthur Cato[1], Marcelo Hayashi[2], Jairo Cavalcante[1], Jonis Qasem[3], Luccas Kavabata[1], Ulisses Costa[1] & Ernani Volpe[1]

[1]University of São Paulo
[2]Federal University of ABC
[3]Technical University of Munich

Abstract

The linearized potential flow theory predicts that the aerodynamic center of thin airfoils at small angles of attack shifts from the quarter–chord point in the subsonic regime to the half–chord point in supersonic flows. However, this linearized theory is not valid for transonic flows and, therefore, it is not possible to predict the correct position of the aerodynamic center analytically in this regime. The goal of this paper is to study the influence of compressibility effects on the aerodynamic center for 2–D airfoils at transonic speeds by means of the continuous adjoint method with an appropriate treatment of boundary conditions. In addition, the theoretical framework of the method is extended to include time dependent flows as well.

Keywords: Adjoint method; aerodynamic center; Euler equations; aerodynamics; CFD.

1. Introduction

Over the past twenty years the adjoint method has been consolidated as one of the most versatile and successful tools for aerodynamic design [7, 10]. It has become a research area on its own, spawning a large variety of applications and a prolific literature. The use of the adjoint method in rotating machinery [13], surface design [8, 9], refinement of meshes [11, 12], etc. proves its potential as optimization tool. Yet, some relevant aspects of the method seem to have remained relatively less explored. Such is the case with the adjoint boundary problem. In particular for Euler flows, both fluid dynamic and adjoint equations entail complementary Riemann problems, and these yield boundary conditions that are fully consistent with well–posedness.

This work takes full advantage of that complementarity on using characteristics–based boundary conditions to solve the adjoint problem. On doing so, it enables one to use a single adjoint solution to compute sensitivity gradients in a more general framework, that is, with respect to both geometric and non–geometric control parameters. It is worth noting that the usual homogeneous adjoint boundary conditions at far–field boundaries would not allow this kind of application. One of the main objectives of the research is to use the method as a reliable and cost–effective tool to evaluate stability derivatives.

2. Control theory for General Systems

This section aims to briefly present the control theory for general systems. It is based on [1], however the time-dependency is considered throughout the text. Although the results for the aerodynamic center shift are focused on steady state flows, a general unsteady formulation is discussed in order to present the theoretical basis developed by the authors.

Consider the system of n-PDE's subject to boundary conditions $\mathbf{B}$. They can be represented in the operator form given by equation (1).

$$\begin{aligned} \mathbf{N}\left[\mathbf{Q}\left(\chi,t\right),\mathbf{P}\right] &= \mathbf{R}\left(\chi,\mathbf{P}\right) \\ \mathbf{B}\left[\mathbf{Q}\left(\chi,t\right),\mathbf{P}\right]_s &= 0 \end{aligned} \tag{1}$$

The vector $\mathbf{Q}$ represents the coordinates in the state space of a point χ from the phase space. The vector $\mathbf{P}$ contains the set of control parameters.

$$\begin{aligned}\mathbf{Q}(\chi) &= [Q_1(\chi),...,Q_n(\chi)]\\ \mathbf{P}(\chi) &= [P_1(\chi),...,P_m(\chi)]\\ \chi &= (\chi_1,...,\chi_i)\end{aligned} \tag{2}$$

The traditional approach used on design problems relies on writing the system of PDE's as function of the control parameters; usually, they correspond to the geometric parameters of the aerodynamic surface. However, one can notice that the boundary condition operator $\mathbf{B}$ is also explicitly written as a function of $\mathbf{P}$ in this work. The idea behind it is to expand the types of control parameters that can be chosen, in other words, it opens up the possibility to compute non-geometric sensitivities associated to physical parameters at the permeable boundaries (e.g. temperature, pressure etc.).
The measure of merit to be improved in aerodynamics is usually described as an integral of the flow variables over the surface. In unsteady flows, the functional can be evaluated as a time-average over a certain period $T = t_f - t_o$ as in equation (3).

$$I[\mathbf{Q},\mathbf{P}] = \frac{1}{T}\int_{t_0}^{t_f}\int_{\chi}\mathscr{F}[\mathbf{Q}(\chi,t),\mathbf{P}(\chi,t),\chi]\,d\chi dt \tag{3}$$

The first variation of the measure of merit yields:

$$\delta I = \frac{1}{T}\left[\int_{t_0}^{t_f}\int_{\chi}\mathscr{F}'_{\mathbf{Q}}\delta\mathbf{Q}d\chi dt + \int_{t_0}^{t_f}\int_{\chi}\mathscr{F}'_{\mathbf{P}}\delta\mathbf{P}d\chi dt\right] \tag{4}$$

The first and second terms of the RHS are usually denoted, respectively, as $\delta I_{\mathbf{Q}}$ and $\delta I_{\mathbf{P}}$. The term $\delta I_{\mathbf{P}}$ is the variation associated to the parametric change; and it has a closed form for many cases. On the other hand, the term $\delta I_{\mathbf{Q}}$ is more difficult to be computed since $\delta\mathbf{Q}$ is unknown, it depends on the flow solution.
The term $\delta I_{\mathbf{Q}}$ can be computed through different flow simulations. Alternatively, if one is able to guarantee that all the $\delta\mathbf{Q}$ are realizable, then there is no need for additional simulations. In order to do it the governing equations are imposed as constraints to the variational problem with the Lagrande multipliers Φ, Ψ and $\mathbf{a}$. It yields to the augmented functional:

$$G = I[\mathbf{Q},\mathbf{P}] - \langle\Phi,\mathbf{N}-\mathbf{R}\rangle - \langle\Psi,\mathbf{B}\rangle_s - \langle\mathbf{a},\mathbf{P}-\mathbf{P}_0\rangle \tag{5}$$

The second and third terms on the RHS are the constrains originated from the system equations and its boundary conditions. The fourth term restrains the set of control parameters to a given configuration baseline $\mathbf{P_0}$ of prescribed values. The symbol $\langle\cdot,\cdot\rangle$ is the inner product defined as follows:

$$\begin{aligned}\langle\mathbf{F},\mathbf{G}\rangle &= \int_{\Omega}\mathbf{F}\cdot\mathbf{G}d\Omega = \int_{t_0}^{t_f}\int_{\mathscr{D}}\mathbf{F}\cdot\mathbf{G}d\mathscr{V}dt\\ \langle\mathbf{F},\mathbf{G}\rangle_S &= \int_{\partial\Omega}\mathbf{F}\cdot\mathbf{G}d\Omega = \int_{t_0}^{t_f}\int_{S}\mathbf{F}\cdot\mathbf{G}dSdt\end{aligned} \tag{6}$$

One can take the differentials of equations (1) to find a local optimum for the variational problem. From (1):

$$\begin{aligned}\mathbf{L}\delta\mathbf{Q} &= \mathbf{S}\delta\mathbf{P}\\ \mathbf{B}'_{\mathbf{Q}}\delta\mathbf{Q} &= -\mathbf{B}'_{\mathbf{P}}\delta\mathbf{P}\end{aligned} \tag{7}$$

Where $\mathbf{L}\equiv\mathbf{N}'_Q$ and $\mathbf{S}\equiv\mathbf{R}'_\alpha-\mathbf{N}'_\alpha$. One can equally define them in terms of their components:

$$\begin{aligned}L_{kr} &= (N_k)'_{Q_r} \qquad k=1,...,n;\;\; r=1,...,n\\ S_{kr} &= (Q_k)'_{P_r} - (N_k)'_{P_r} \quad k=1,...,n;\;\; r=1,...,m\end{aligned} \tag{8}$$

The first variation of the augmented functional can be computed by taking the Gâteaux variations of each term from equation (5):

$$\begin{aligned}\delta G =& \langle \mathscr{F}'_{\mathbf{Q}}, \delta\mathbf{Q}\rangle + \langle \mathscr{F}'_{\mathbf{P}}, \delta\mathbf{P}\rangle - \langle \delta\Phi, \mathbf{N}-\mathbf{R}\rangle - \langle \Phi, \mathbf{L}\delta\mathbf{Q}\rangle + \\ &+ \langle \Phi, \mathbf{S}\delta\mathbf{P}\rangle - \langle \delta\Psi, \mathbf{B}\rangle_s - \langle \Psi, \mathbf{B}'_{\mathbf{Q}}\delta\mathbf{Q}\rangle_s + \\ &- \langle \Psi, \mathbf{B}'_{\mathbf{P}}\delta\mathbf{P}\rangle_s - \langle \delta\mathbf{a}, \mathbf{P}-\mathbf{P}_0\rangle - \langle \mathbf{a}, \delta\mathbf{P}\rangle\end{aligned} \tag{9}$$

One can integrate by parts the term $\langle \Phi, \mathbf{L}\delta\mathbf{Q}\rangle$:

$$\langle \Phi, \mathbf{L}\delta\mathbf{Q}\rangle = \langle \mathbf{L}^\star\Phi, \delta\mathbf{Q}\rangle - P[\Phi, \delta\mathbf{Q}]_s \tag{10}$$

The expression above introduces the adjoint operator of $\mathbf{L}$, represented by a $\mathbf{L}^\star$. The term $P[\Phi, \delta\mathbf{Q}]_s$ is called bilinear concomitant and it is computed as an inner product; it can be decomposed into two parts:

$$P[\Phi, \delta\mathbf{Q}]_s = \langle P_1(\Phi), \mathbf{B}'_{\mathbf{Q}}\delta\mathbf{Q}\rangle_s + \langle \mathbf{B}^\star(\Phi), \mathbf{M}\delta\mathbf{Q}\rangle_s \tag{11}$$

The first product is between $P_1(\Phi)$ and the linearized boundary operator $\mathbf{B}'_{\mathbf{Q}}\delta\mathbf{Q}$. The second one introduces the adjoint boundary operator $\mathbf{B}^\star(\Phi)$ and $\mathbf{M}\delta\mathbf{Q}$. The operator $\mathbf{M}$ must be linearly independent from $\mathbf{B}'_Q$. It should be highlighted that both the decomposition of the bilinear concomitant and $\mathbf{M}$ are not unique [1]. Finally, δG can be expressed as:

$$\begin{aligned}\delta G =& -\langle \delta\Phi, \mathbf{N}-\mathbf{R}\rangle - \langle \delta\Psi, \mathbf{B}\rangle_s - \langle \delta\mathbf{a}, \mathbf{P}-\mathbf{P}_0\rangle - \langle \mathbf{L}^\star\Phi - \mathscr{F}'_{\mathbf{Q}}, \delta\mathbf{Q}\rangle + \\ &- \langle \Psi, \mathbf{B}'_{\mathbf{Q}}\delta\mathbf{Q}\rangle_s - \left[\langle P_1(\Phi), \mathbf{B}'_{\mathbf{Q}}\delta\mathbf{Q}\rangle_s + \langle \mathbf{B}^\star(\Phi), \mathbf{M}\delta\mathbf{Q}\rangle_s\right] + \langle \Phi, \mathbf{S}\delta\mathbf{P}\rangle + \\ &\langle \mathscr{F}'_{\mathbf{P}}, \delta\mathbf{P}\rangle - \langle \Psi, \mathbf{B}'_{\mathbf{P}}\delta\mathbf{P}\rangle_s - \langle \mathbf{a}, \delta\mathbf{P}\rangle\end{aligned} \tag{12}$$

And for the local optimums of the augmented functional:

$$\delta G = 0 \;\; \forall\{\delta\mathbf{Q}, \delta\mathbf{P}, \delta\Phi, \delta\Psi, \delta\mathbf{a}\} \in \{\textit{locus} \text{ of realizability}\} \tag{13}$$

As explained in [1], the following condition have to be achieved:

1. The governing equations are satisfied along with the specified boundary conditions as in (1). The parameter vector corresponds to the baseline configuration $\mathbf{P} = \mathbf{P}_0$. This implies in the annulment of the three first terms from equation (12).

2. If
$$\Psi = -P_1(\Phi) \tag{14}$$
then the fifth and sixth terms are cancelled and the vector Ψ can be written in function of Φ.

3. The adjoint equation and the adjoint boundary conditions are satisfied for Φ:
$$\begin{aligned}&\mathbf{L}^\star\Phi - \mathscr{F}'_{\mathbf{Q}} = 0 \\ &\mathbf{B}^\star(\Phi) = 0\end{aligned} \tag{15}$$

4. The vector $\mathbf{a}$ is given by:
$$\langle \mathbf{a}, \delta\mathbf{P}\rangle = \langle \Phi, \mathbf{S}\delta\mathbf{P}\rangle + \langle \mathscr{F}'_{\mathbf{P}}, \delta\mathbf{P}\rangle - \langle \Psi, \mathbf{B}'_{\mathbf{P}}\delta\mathbf{P}\rangle_s \tag{16}$$
which gathers the remaining terms when $\delta G = 0$.

The last condition gives the realizable part of the sensitivity gradient, meaning $\langle \mathbf{a}, \delta\mathbf{P}\rangle = \delta I$. The proof of this statement can be found in [1].

3. Time-dependent Adjoint Method applied to Compressible Euler Equations

The further development is an extension of the work done in [4] and [3]. The adjoint method is applied to the Euler equations as formulated in the previous section; however, one can notice two generalizations presented here which are different from the previous cited works: first, the method is applied to the time-dependent Euler equations; second, the control parameters can be associated with the inflow and outflow boundaries. The former consideration leads to a time-dependent adjoint method and the latter one allows one to compute sensitivities with respect to parameters at the outflow and not only at the inflow.

Equation (17) represents the Euler equations in a general system of coordinates ξ^k.

$$\frac{\partial \left(JQ_\alpha\right)}{\partial t} + \frac{\partial F_\alpha^k}{\partial \xi^k} = 0 \tag{17}$$

Where J is the transformation Jacobian for different coordinates. The state vector Q_α and the flux vector $f_\alpha^{k'}$ are:

$$Q_\alpha \Rightarrow \begin{pmatrix} \rho \\ \hline \rho u^{i'} \\ \hline e \end{pmatrix} \; ; \; f_\alpha^{k'} \Rightarrow \begin{pmatrix} \rho u^{k'} \\ \hline \rho u^{i'k'} + p g^{i'k'} \\ \hline \left(e+p\right) u^{k'} \end{pmatrix} \tag{18}$$

Where $e = \rho\left(e_i + \frac{\mathbf{u}\cdot\mathbf{u}}{2}\right)$ and e_i is the specific internal energy, and $g^{i'k'}$ is the metric tensor, which is the identity matrix in Cartesian coordinates.

One can write the augmented functional as:

$$G = \underbrace{\frac{1}{T}\int_{t_0}^{t_f}\int_{b_w} \mathscr{F}\left[\mathbf{Q},\mathbf{P}\right]\left|\frac{dS'}{dS}\right| dS dt}_{I} + \underbrace{\left\langle \phi_\alpha, \frac{\partial \left(JQ_\alpha\right)}{\partial t} + \frac{\partial F_\alpha^k}{\partial \xi^k}\right\rangle}_{I_1} + \underbrace{\langle \psi, \mathbf{B}\rangle_s}_{I_2} + \underbrace{\langle \mathbf{a}, \mathbf{P}-\mathbf{P}_0\rangle}_{I_3} \tag{19}$$

The term denoted by I is the measure of merit and it is written explicitly in a integral to highlight the fact that it is a time-averaged measure; the ratio of areas $\frac{dS'}{dS}$ shows the change of coordinates and the subscript b_w stands for the wall boundary. By proceeding as described before, the variation of the augmented functional can be written for the unsteady Euler equations:

$$\begin{aligned}
\delta G = & \underbrace{\left\langle \delta\phi_\alpha, \frac{\partial \left(JQ_\alpha\right)}{\partial t}\right\rangle + \left\langle \delta\phi_\alpha, \frac{\partial F_\alpha^k}{\partial \xi^k}\right\rangle + \langle \delta\psi, \mathbf{B}\rangle_s + \langle \delta\mathbf{a}, \mathbf{P}-\mathbf{P}_0\rangle +}_{\text{(I) Physical problem}} \\
& \underbrace{-\left\langle \frac{\partial \phi_\alpha}{\partial t}, \left(J\delta Q_\alpha\right)\right\rangle - \left\langle \frac{C_{\alpha\beta}^k}{J}\frac{\partial \left(J\phi_\alpha\right)}{\partial \xi^k}, \delta Q_\beta\right\rangle +}_{\text{(II) Adjoint equation}} \\
& \underbrace{\left\langle \psi_\alpha \frac{\partial B_\alpha}{\partial Q_\beta} + \phi_\alpha C_{\alpha\beta}^k n_k, \delta Q_\beta\right\rangle_{s_i} + \left\langle \psi_\alpha \frac{\partial B_\alpha}{\partial Q_\beta} + \phi_\alpha C_{\alpha\beta}^k n_k, \delta Q_\beta\right\rangle_{s_o} +}_{\text{(III) Adjoint boundary conditions}} \\
& \underbrace{\left\langle \frac{\partial \mathscr{F}}{\partial Q_\alpha}\left|\frac{dS'}{dS}\right| + \frac{\partial p}{\partial Q_\alpha}\left[\phi_{i'+1} J \beta_{i'}^2 n_2\right], \delta Q_\alpha\right\rangle_{b_w}}_{\text{(III) Adjoint boundary conditions}} + \underbrace{\left[\int_\Omega \phi_\alpha \left(J\delta Q_\alpha\right) d\Omega\right]_{t_0}^{t_f}}_{\text{(IV) Time condition}} + \\
& \underbrace{\left[\left\langle \phi_\alpha, \delta\left(J\beta_{i'}^k\right) f_\alpha^{i'} n_k\right\rangle_{s_i} + \left\langle \phi_\alpha, \delta\left(J\beta_{i'}^k\right) f_\alpha^{i'} n_k\right\rangle_{s_o}\right]_{=\text{farfield}} + \left\langle \mathscr{F}, \delta\left|\frac{dS'}{dS}\right|\right\rangle_{b_w} +}_{\text{(V) Adjoint gradient}} \\
& \underbrace{\left\langle \phi_\alpha, \frac{\partial \left(Q_\alpha \delta J\right)}{\partial t}\right\rangle - \left\langle \delta\left(J\beta_{i'}^k\right), \frac{f_\alpha^{i'}}{J}\frac{\partial \left(J\phi_\alpha\right)}{\partial \xi^k}\right\rangle + \langle p, \left[\phi_{i'+1}\delta\left(J\beta_{i'}^2\right) n_2\right]\rangle_{b_w} +}_{\text{(V) Adjoint gradient}} \\
& \underbrace{\langle \psi, \mathbf{B}'_{\mathbf{P}}\delta\mathbf{P}\rangle_s + \langle \mathbf{a}, \delta\mathbf{P}\rangle}_{\text{(V) Adjoint gradient}}
\end{aligned} \tag{20}$$

As it can be seen, the final form of equation (20) is slightly different from the previous works [4, 3]. In equation (20), $\beta_{i'}^{k}$ is the transformation between Cartesian and transformed space, $C_{\alpha\beta}^{k}$ are the generalized Jacobian flux matrices, $f_{\alpha}^{i'}$ is the flux vector in Cartesian coordinates. Each set of terms in this equation characterises a determined part of the overall problem. Particularly, the term (V) consists of the sensitivity gradient. If one wants to compute the sensitivities related to the inflow and outflow with no geometry variations, term (V) becomes simply:

$$\langle \mathbf{a}, \delta\mathbf{P} \rangle = \begin{cases} -\langle \psi, \mathbf{B}'_{\mathbf{P}} \delta\mathbf{P} \rangle_{s_i} & \text{(sensitivity with respect to an inflow parameter)} \\ -\langle \psi, \mathbf{B}'_{\mathbf{P}} \delta\mathbf{P} \rangle_{s_o} & \text{(sensitivity with respect to an outflow parameter)} \end{cases} \tag{21}$$

4. Adjoint Contour Problem

Some novel developments have been built on what was accomplished in [4, 3] and, hence, on what was originally proposed for the present work. The adjoint Euler problem has since been extended to time–dependent flows, and to evaluate the sensitivity with respect to the outflow boundary condition, namely the static pressure on that boundary. Now both inflow and outflow boundary conditions can be parameterized, controlled and time-dependent. We are, as yet, in the process of implementing these new resources in the computation of stability derivatives. Nonetheless, we have decided to discuss their derivation in what follows, and to include a simple, yet illustrative application of it in Sec. 5.2

4.1 Time Conditions

The time condition comes from the annulment of term (IV) in equation (20). It is presented below:

$$(\text{IV}) = \left[\int_{\Omega} \phi_{\alpha} \left(J \delta Q_{\alpha} \right) d\Omega \right]_{t_0}^{t_f} = 0 \tag{22}$$

It is interesting to work with the adjoint problem in terms of the variable $t^{\star} = t_f - t$, which can be associated with a reversion in time. Consequently, the adjoint equations given in terms of $t^{\star}$ have an hyperbolic behavior complementary to the Euler's equations, where their difference lies in the signal of the convective term.

As the initial condition of the physical problem is imposed, one can see that $\delta Q_{\alpha}|_{t_0} = 0$. Due to equation (22), the volume integral at time t_f is also null. As $t_0^{\star} = t_f$ and $t_f^{\star} = t_0$, the initial condition of the adjoint equation is simply:

$$\phi_{\alpha}\big|_{t_f = t_0^{\star}} = 0 \ \text{ everywhere} \tag{23}$$

The initial condition of the adjoint problem corresponds to the final condition of the physical problem.

4.2 Boundary Conditions

The adjoint boundary conditions for steady flows are discussed in the works [6, 2, 4, 3]. Unsteady flows are subject to the exact same adjoint boundary conditions [3], with the only change that one must integrate them in reverse time as well. To that end, one must keep track of the whole time evolution of the physical problem. In this work we introduce the appropriate form for active control of the outflow boundary, which is presented below.

The number of conditions imposed depends on the flow regime and, therefore, they are analyzed separately. For the supersonic outlet, there are four physical characteristics (in two dimensions) that travel from the inside to the outside of the domain; thus, four adjoint characteristics travel from the outside to the inside. There are four adjoint conditions to be imposed [4]:

$$\varphi_i|_{s_o} = 0 \tag{24}$$

One physical condition must be imposed at the subsonic outlet. On the other hand, three adjoint conditions must be imposed and one is determined by the flow solution in the interior of the domain. The static pressure is usually chosen as the outlet condition and it can be described by a function controlled through the parameters P_p^k:

$$\text{Outlet property} \left\{ p = f_p \left(x, y, z, t, P_p^k \right) \right. \tag{25}$$

The static pressure can be written in terms of the primitive variables $\mathbf{Q_1}$, $\mathbf{Q_2}$, $\mathbf{Q_3}$ and $\mathbf{Q_4}$. The linearized form of this function can be presented in the convenient matrix form of equation (26).

$$\underbrace{\begin{bmatrix} 0 & 0 & 0 & 0 \\ 0 & 0 & 0 & 0 \\ 0 & 0 & 0 & 0 \\ \frac{\left(u^2+v^2\right)}{2} & -u & -v & 1 \end{bmatrix}}_{\mathbf{B'_Q}} \underbrace{\begin{bmatrix} \delta Q_1 \\ \delta Q_2 \\ \delta Q_3 \\ \delta Q_4 \end{bmatrix}}_{\delta \mathbf{Q}} = - \underbrace{\begin{bmatrix} 0 \\ 0 \\ 0 \\ \frac{1}{\gamma-1}\frac{\partial f_p}{\partial P_p} \end{bmatrix}}_{\mathbf{B'_P}} \underbrace{\left[\delta P_p\right]}_{\delta \mathbf{P}} \tag{26}$$

The matrix $\mathbf{B'_Q}$ is essentially the same as the one found in [4]. The interesting fact is that, although that work did not consider a controlled outlet, one could apply the same adjoint boundary condition from that reference. The boundary condition for the geometric case can be used for the present one:

$$\begin{cases} \varphi_1 - C_1\varphi_4 = 0 \\ \varphi_2 - C_2\varphi_4 = 0 \\ \varphi_3 - C_3\varphi_4 = 0 \end{cases} \tag{27}$$

The coefficients C_i depend on flow properties at time $t = t_f - t^\star$. In terms of operator, the adjoint boundary conditions can be translated as:

$$\mathbf{B}^\star = \begin{bmatrix} 1 & 0 & 0 & -C_1 \\ 0 & 1 & 0 & -C_2 \\ 0 & 0 & 1 & -C_3 \\ 0 & 0 & 0 & 0 \end{bmatrix} \tag{28}$$

The gradient with respect to an outflow parameter can be computed substituting the $\mathbf{B'_P}$ from equation (26) in equation (21).

5. Results

The adjoint problem thus formulated is used to compute the derivatives of the lift and pitching moment with respect to the angle of attack for different Mach numbers. The airfoils profiles used are the NACA 0012 and RAE 2822. The present approach allows one to find the aerodynamic center shift according to the Mach number.

The sensitivity gradients for steady flows are compared to their finite differences counterparts, in a validation procedure that is similar to that presented in previous works. The adjoint method proposed for steady state cases and the code used are validated in [5, 6, 2, 4, 3]. A test case for the time dependent formulation of the adjoint method for non-geometric parameters is included at the end of the section.

5.1 Aerodynamics Center Shift

This approach opens up the possibility of employing the adjoint method to assess the sensitivity of a given measure of merit with respect to changes in aerodynamic variables as the Mach number, in addition to the usual geometry–design applications. Figure 1 shows, for instance, gradients of nondimensional lift, L, and pitching moment about the leading edge, M_{le}, with respect to the angle of attack, α, for the NACA 0012 profile at zero angle of attack, as functions of the far–field Mach numbers. The values of the gradients were also computed with finite differences for the values of Mach 0.5, 0.6, 0.7, 0.8, 0.9 and 1.0.

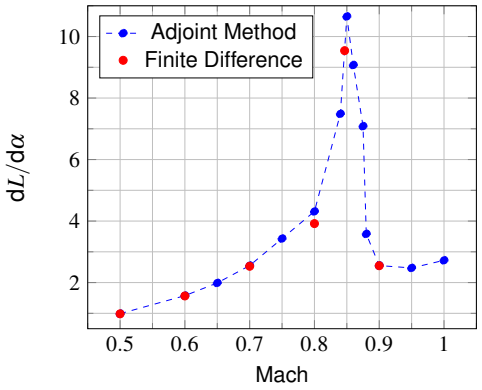

(a) Gradient of the nondimensional lift with respect to the angle of attack.

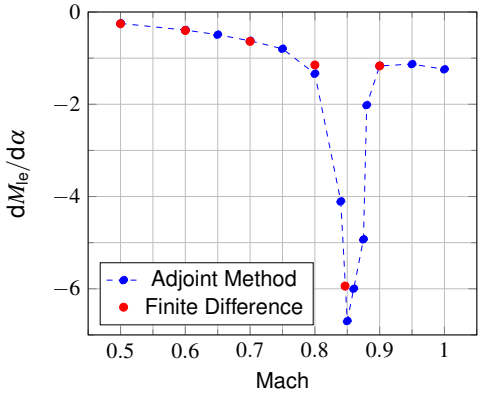

(b) Gradient of the nondimensional pitching moment about the leading edge with respect to the angle of attack.

Figure 1 – NACA 0012: Sensitivities with respect to the angle of attack.

The continuous adjoint method shows agreement with the finite differences as expected. One of the advantages of the adjoint method is the lower number of simulations it entails; one must do four simulations to compute one point of $\frac{dL}{d\alpha}$ and one point of $\frac{dM}{d\alpha}$ with FD, while the same points can be found with three simulations using the adjoint method (the flow solution and two adjoint solutions according to the measure of merit chosen). In problems with a great number of parameters, the FD method can become impracticable.
Analogous results are plotted for the RAE 2822 in figures 2a and 2b.

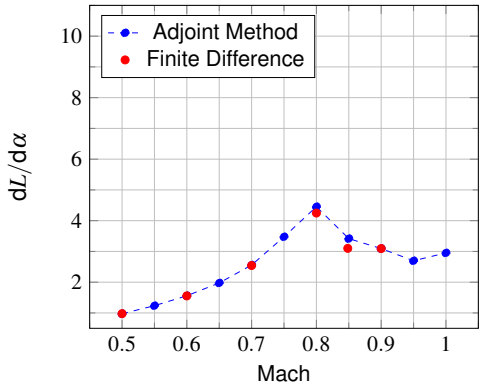

(a) Gradient of the nondimensional lift with respect to the angle of attack.

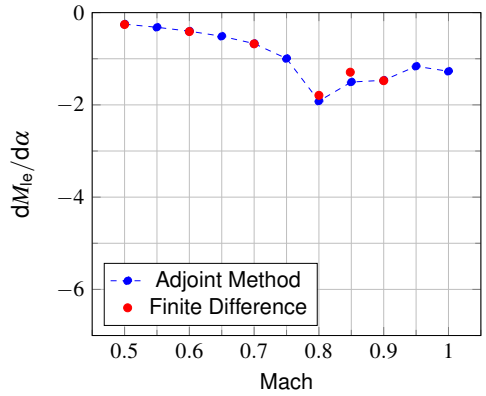

(b) Gradient of the nondimensional pitching moment about the leading edge with respect to the angle of attack.

Figure 2 – RAE 2822: Sensitivities with respect to the angle of attack.

Note that those sensitivities, given by the adjoint computations, enable one to determine the aerodynamic center position, x_{ac}, of the airfoil by the expression:

$$\frac{x_{\text{ac}}}{c} = -\frac{(\mathrm{d}M_{\text{le}}/\mathrm{d}\alpha)}{(\mathrm{d}L/\mathrm{d}\alpha)} \tag{29}$$

where c is the chord of the airfoil.
Figure 3a shows the aerodynamic center shift for the NACA 0012 profile obtained by equation (29) and the results from figure 1. It is worth noting also that, on using this approach, it is possible to obtain the sensitivity of the aerodynamic center position with respect to the far–field Mach number. The aerodynamic center shift is also computed from the finite differences results. Figure 3b shows the aerodynamic center for the RAE 2822.

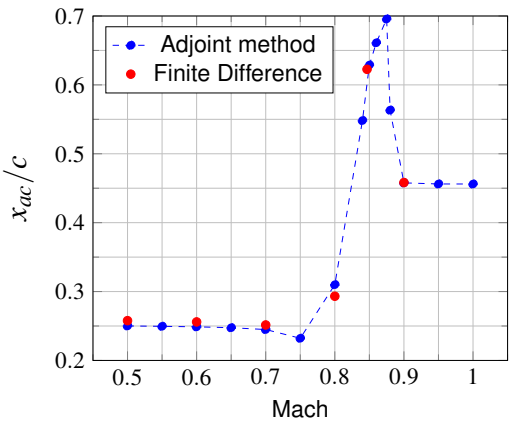

(a) Aerodynamic center shift of the NACA 0012 profile in transonic flow regime.

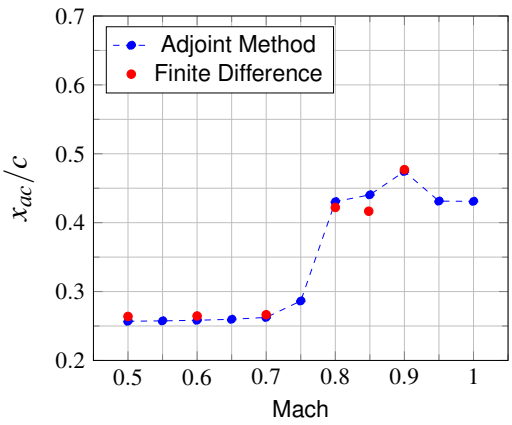

(b) Aerodynamic center shift of the RAE 2822 profile in transonic flow regime.

Figure 3 – Aerodynamic center shift of different airfoils in transonic flow regime.

5.2 Time-dependent case

A first result of the unsteady adjoint method for non-geometric parameters is presented. A totally divergent supersonic nozzle with the geometry used in [4] is considered due to its simplicity for a preliminary test case. A steady state solution is computed with the inlet conditions given in table 1 and the outlet condition in table 2.

Table 1 – Inlet initial conditions for subsonic flow

Inlet Conditions (non-dimension)	
Total Pressure	1.01
Total Temperature	0.75
Inlet Angle	0.0

Table 2 – Outlet initial condition for subsonic flow

Outlet Conditions (non-dimension)	
Pressure	0.95

This solution is used as initial condition for the time-dependent case. From there, the inlet total pressure becomes a function of time and it can be written as $p_o(t) = p_{o_i} + A \cdot p_{o_i} \cdot \sin \omega t$, where p_{o_i} is the initial total pressure, A is the amplitude of oscillation and ω is the frequency. These are the control parameters of the function. The total pressure is plotted for some frequencies in figure 4.

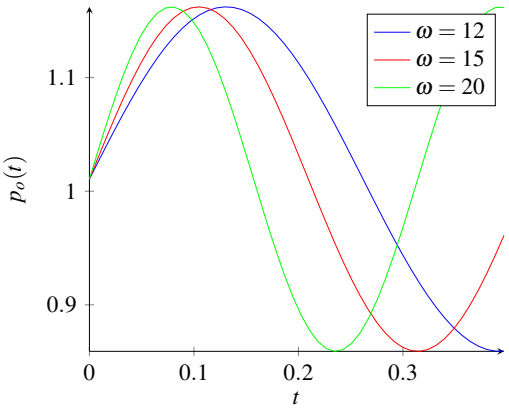

Figure 4 – Inlet stagnation pressure for different frequencies

All the values, including time, are given in non-dimensional form defined as:

$$\begin{aligned} \rho^+ &= \frac{\rho}{\rho_\infty} \qquad l^+ = \frac{l}{l_0} \qquad u_i^+ = \frac{u_i}{c_\infty} \qquad p^+ = \frac{p}{\rho_\infty c_\infty^2} \\ t^+ &= \frac{c_\infty}{l_0} t \qquad T^+ = \frac{T}{T_\infty} \qquad e^+ = \frac{e}{\rho_\infty c_\infty^2} \end{aligned} \tag{30}$$

The measure of merit chosen is the non-dimensional lateral force applied to the nozzle wall and integrated over a given time interval $T \approx 0.4$. The sensitivity of the measure of merit with respect to the frequency of the inlet total pressure is then computed with both adjoint method and FD. Figure 5a presents the pressure distribution at $t \approx 0.2385$ for $\omega = 20$ and figure 5b presents Ψ_1 at the corresponding $t^\star \approx 0.1582$.

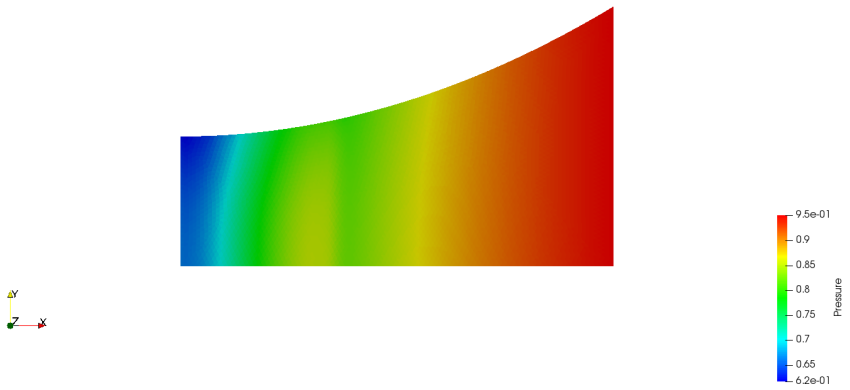

(a) Pressure at $t \approx 0.2385$

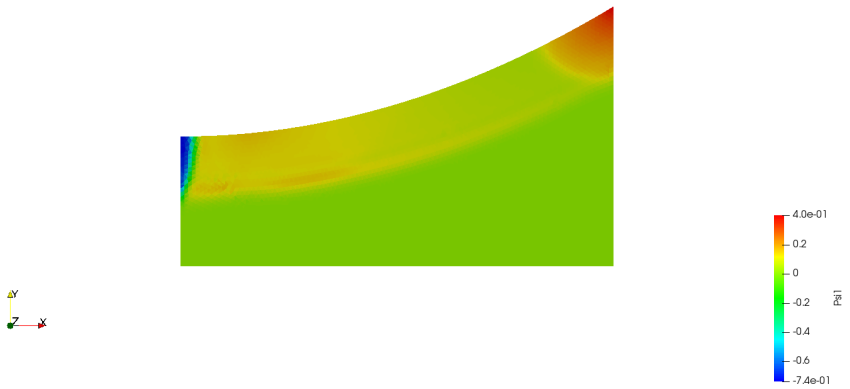

(b) Ψ_1 at $t^\star \approx 0.1582$

Figure 5 – Subsonic divergent nozzle

The computed derivative $\frac{\partial I}{\partial \omega}$ is shown in figure 6. Both results from FD and the time-dependent adjoint method agree. In conclusion, some important aspects should be highlighted: the method proposed can be applied to both internal and external flows; the physical initial condition is computed as solution of a steady state flow, in other words, it belongs to the space of realizable flows and the gradient of the time-averaged functional can be computed for an arbitrary time starting from this point (as long as the solution is time accurate); as the adjoint solution depends on the physical solution at each time step, the latter one needs to be saved entirely (or it must contain enough information for its reconstruction).

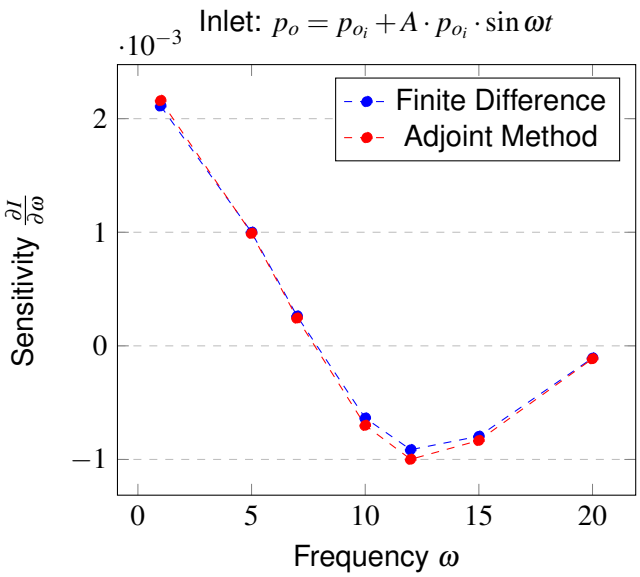

Figure 6 – Sensitivity of I with respect to the oscillation frequency ω of the inlet total pressure (subsonic case)

6. Conclusion

The adjoint method used to compute gradients with respect to geometric parameters is a current tool in aerodynamic shape optimization problems; however, its use can be extended to non-geometric parameters as well. The present work shows its capability to compute the aerodynamic center shift for different airfoils with respect to the Mach number. The study indicates that the method can provide reliable results when compared to the finite differences approach with the advantage of less simulations.

The development of the time-depend continuous adjoint method for non-geometric parameters is also developed in the framework of this study. The preliminary results concerning a test case simulation is used as a first validation of the method. Although the method is applied to an internal flow, it can be used to external flows as well. The main difficult lies in the large data storage capacity that is required to keep the whole time evolution of both flow and adjoint solutions.

References

[1] Cacuci et al. *Sensitivity theory for general systems of non–linear equations*. In: *Nuclear Science and Engineering* 75 (1980), pp. 88–110.

[2] Hayashi, M., Ceze, M., and Volpe, E. *Characteristics-based boundary conditions for the Euler adjoint problem*. In: *Int. J. Numer. Meth. Fluids* 71.10 (Apr. 2013), pp. 1297–1321. ISSN: 1097–0363. DOI: 10.1002/fld.3712. URL: https://doi.org/10.1002/fld.3712.

[3] Hayashi, M., Ceze, M., and Volpe, E. *On the use of the continuous adjoint method to compute non–geometric sensitivities*. In: *Int. J. for Numer. Meth. Fluids* 86.11 (2018). fld.4473, pp. 679–698. ISSN: 1097–0363. DOI: 10.1002/fld.4473. URL: http://dx.doi.org/10.1002/fld.4473.

[4] Hayashi, M. et al. *Non–geometric sensitivities using the adjoint method*. In: *ICAAA2016*. Vol. 10. 1. World Academy of Science Engineering and Technology. London, UK: International Scholarly, Scientific Research, and Innovation, Jan. 2016, pp. 155–163.

[5] Hayashi, M. T. *Estudo conceitual do problema adjunto baseado nas equações de Euler para aplicações de otimização aerodinâmica*. In: São Paulo, SP, Brasil, 2009.

[6] Hayashi, M. T., Ceze, M. A. B., and Volpe, E. V. *Characteristics–based boundary conditions for the Euler adjoint problem: 2–D formulation*. In: *AIAA Applied Aerodynamics Conference*. 2010–4677. AIAA. Chicago, IL, June 2010.

[7] Jameson, A. *Aerodynamic design via control theory*. In: *12th IMACS World Congress on Scientific Computation*. Paris, 1988.

[8] Jameson, A. *Optimum aerodynamic design using control theory*. In: *Computational Fluid Dynamics Review*. Annual Book Series (1995), 495–528.

[9] Martins, J. R. R. A., Alonso, J. J., and Reuther, J. J. *A coupled–adjoint sensitivity analysis method for high–fidelity aero–structural design*. In: *Optimization and Engineering* 6 (2005), 33–62.

[10] Reuther, J. J. and Jameson, A. *Aerodynamic shape optimization of wing and wing–body configurations using control theory*. In: *AIAA. 33rd Aerospace Sciences Meeting and Exhibit. AIAA Paper 95-0123*. 1995.

[11] Venditti, D. A. and Darmofal, D. L. *A multilevel error estimation and grid adaptive strategy for improving the accuracy of integral outputs*. In: *AIAA Paper*. 99–3292. AIAA. 1999.

[12] Venditti, D. A. and Darmofal, D. L. *Grid adaptation for functional outputs: Application to two-dimensional inviscid flows*. In: *Journal of Computational Physics* 176 (2002), 40–69.

[13] Walther et al. *Constrained adjoint-based aerodynamic shape optimization of a single-stage transonic compressor*. In: *ASME Journal of Turbomachinery* (July 2012). DOI: 10.1115/1.4007502.

Copyright Statement